



Effect of ursodiol on alginate/PLL nanoparticles with non-ionic surfactant for gene delivery

Thomas Foster · Patrick Lim · Bozica Kovacevic ·
Susbin Raj Wagle · Corina Mihaela Ionescu ·
Armin Mooranian · Hani Al-Salami

Received: 14 November 2023 / Accepted: 22 January 2024 / Published online: 20 February 2024
© The Author(s) 2024

Abstract Hearing loss is a widespread condition, affecting people from a range of demographics. Gene therapy is an emerging method for the amelioration of this condition. Challenges associated with the delivery of genes to various sites within the ear remain a significant challenge. In the present work, a novel polymer nanoparticle delivery system was developed, incorporating a bile acid excipient. Bile

acids have previously been shown to improve drug delivery through their permeation enhancing properties; however, few studies report their use in gene delivery systems. Nanoparticles were developed with sodium alginate and poly-L-lysine through an ionotropic gelation method. Various surfactants including Tween-80 and poly-ethylene glycol 6000 were incorporated to both improve the solubility of the bile acid, ursodiol, and to modify nanoparticle properties. The evaluation of the nanoparticle's safety profiles was the primary outcome of this study. The secondary aims were to perform genetic studies, such as transfection efficiency. The nanoparticles generated in this study demonstrated formulation-dependent variability in particle size ranging from 30 to 300 nm. Several of the developed formulations demonstrated suitable safety profiles; further, the introduction of bile acid helped to reduce toxicity. Transfection efficiency for all formulations remained low, potentially due to poor plasmid release inside the cell. Poor transfection efficiency is one of the key pitfalls associated with polymer nanoparticles. Overall the present study developed nanoparticles with suitable safety profiles but limited efficacy. The use of modified polymers, additional excipients, and cell-targeting peptides are potential methods that may be explored in future studies to help further improve gene delivery.

Armin Mooranian and Hani Al-Salami equally contributing corresponding authors.

T. Foster · P. Lim · B. Kovacevic · S. R. Wagle ·
C. M. Ionescu · A. Mooranian (✉) · H. Al-Salami (✉)
The Biotechnology and Drug Development Research
Laboratory, Curtin Medical School & Curtin Health
Innovation Research Institute, Curtin University, Bentley,
Perth, WA 6102, Australia
e-mail: a.mooranian@curtin.edu.au

H. Al-Salami
e-mail: Hani.Al-Salami@curtin.edu.au

T. Foster
Department of Clinical Biochemistry, Pathwest Laboratory
Medicine, Royal Perth Hospital, Perth, WA 6000, Australia

A. Mooranian
School of Pharmacy, University of Otago,
Dunedin, Otago 9016, New Zealand

H. Al-Salami
Medical School, University of Western Australia, Perth,
WA 6000, Australia

Keywords Gene therapy · Nanotechnology ·
Hearing loss · Bile acid · Polymer · Nanobiomedicine

Introduction

Hearing loss places a significant burden on society. It is reported that 1 in 5 people globally suffer from some degree of hearing loss [1], with an economic burden of \$USD750 billion [2]. To date, pharmaceutical interventions have shown limited success. Alternative techniques, including the use of gene therapy, represent an emerging field of hearing loss treatment [3]. Gene therapies represent one of the most significant options in this field [4]. One commonly employed strategy relies on the delivery of specific gene-containing vectors to the supporting cells of the inner ear [5]. These supporting cells will then gain function to differentiate into functional hair cells that will, ideally, restore hearing function [6]. There are however several challenges associated with the delivery of genetic material to the inner ear. These include difficulty in reaching cells of interest, invasive procedures, presence of nuclease, membrane permeation, off-target effect, and poor efficacy [7, 8]. Accordingly, delivery vehicles, both viral and non-viral have been proposed as logical means to improve inner ear gene delivery [9]. Both methods act to protect the plasmid and to effectively deliver it to a site of interest. Although there has been significant interest in viral vectors for inner ear gene therapy [10], there are significant risks that make non-viral delivery methods potentially more viable.

Here, we describe the development of a novel, non-viral, polymeric nanoparticle system for the *in vitro* delivery of a green fluorescent protein (GFP) to an inner ear cell line. Previous studies have discussed the development of ionotropically gelled sodium alginate (SA)/poly-L-lysine (PLL) nanoaggregates for nucleotide delivery [11, 12]. GFP acts as an analogue for a potential gene of interest that may be applied to the inner ear. In this way, this technology may be more versatile in which genes it can deliver. Several genes including *Atoh1*, *Sox2*, *Six1*, and *Eya1* have been implicated as potential candidates either alone or in combination to induce supporting cell differentiation into functional hair cells [13–16]. Ideally, future studies will explore the effects of delivering these and similar genes.

Bile acids have shown significant potential as delivery adjuncts for cells and drugs [17–20]. Limited research has explored bile acid's potential in

modifying gene delivery, especially to the inner ear [21]. To date, no significant studies have reported the use of the secondary bile acid ursodeoxycholic acid (UDCA) in the delivery of genes. UDCA is used widely therapeutically, sometimes referred to as ursodiol and has been shown to have numerous beneficial pharmaceutical effects [22–26]. UDCA is however extremely poorly water-soluble [27]. There have been several proposed methods to improve its solubility, including complexing with cyclodextrins [28], the addition of urea or mannitol [29], and the use of various surfactants [30]. In the present study, UDCA was solubilised through the addition of surfactants, including Tween-80 and polyethylene glycol (PEG) and ethanol. Some studies report that surfactants, including Tween-80 result in the reduction of particle size of SA-based nanoparticles [31]. It is thought that the surfactant decreases SA nanoparticle surface tension thereby increasing the dispersion of alginate into smaller particles [32]. Accordingly, the influence of Tween-80 + UDCA and Tween-80 alone will be reviewed. Bile acids have also shown, in addition to their therapeutic effects, the ability to improve the permeation of particles across membranes [33–36]. Improved permeation due to bile acids has also been suggested to have the potential to occur within the inner ear [37].

Accordingly, this study explored SA-based nanoparticles formed via ionotropic gelation. Formulations were prepared to review the impact of UDCA solubilised in the non-ionic surfactant Tween-80. The primary outcome of this study was exploring the changes in cellular health between these formulations on the inner ear cell line, HEI-OC1. Qualitative assessments of gene expression were also a primary outcome of this study.

Methods and materials

Nanoparticle preparation

Stock solutions of SA, bile acid, CaCl_2 , and PLL were prepared at 0.01 mg/ml. SA stock (sodium alginate, low molecular weight, Sigma-Aldrich, USA) was first diluted further in Milli-Q water. A pre-gel was then formed with the addition of CaCl_2 (calcium chloride dihydrate, 99% MW = 147.02, Thermo Fisher, USA)

under constant stirring. A CaCl_2 :SA (w:w) ratio of 0.2 was used to prepare all formulations in this study. Several techniques were explored to attempt to increase the solubility of UDCA from Sigma-Aldrich (USA). Formulations of 1% Tween-80 (Sigma-Aldrich, USA), 5% Tween-80, 10% Tween-80, 1% Tween-80+5% ethanol, 5% ethanol, 5% polyethylene glycol (PEG) 600 diacid (Sigma-Aldrich, Germany), and 5% PEG 600 diacid+5% ethanol were trialed. The various formulation solubilising agents are shown in Fig. 1. Solutions were filtered through a 0.22 μm filter (Millipore Express PES membrane filter Unit, Merck Millipore, Cork, Ireland) to reduce any aggregates. The UDCA solution was then added (except in the control formulation), and the solution was allowed to homogenise over 10 min. Dilute PLL (Sigma-Aldrich, USA) was then added to produce ionic gelation of the nanoparticles. A SA: PLL (w:w) ratio of 1.5 was used in this study for all formulations. The particles were then mixed for at least 60 min at 1000 RPM. The final solution volume was 4 ml. Formulation 1 contained neither Tween-80 nor bile acid, whilst formulation 2 contained Tween and no bile acid.

Nanoparticles were prepared without cryoprotectant before being frozen overnight at -80°C , and subsequently freeze-dried in the Scanvac Cool-safe Freeze Drier for 48–96 h or until it appeared that there was no more moisture remaining. For cellular studies, the nanoparticles were reconstituted

and used within 48 h. Particles were filtered through a 0.22- μm filter prior to use in further experiments.

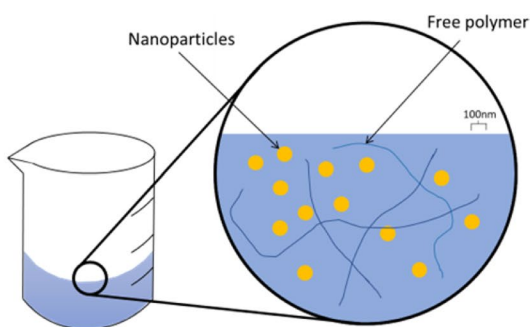
Structural analysis

Nanoparticle size, charge, and PDI were measured via dynamic light scattering technology. Analysis was performed on the Zetasizer 3000HSa (Malvern, UK), as per previously established methods [17, 38]. Briefly, a refractive index of 1.33 with an absorption of 0.1 was used for detection. The dispersant was set to water, with a viscosity of 0.8872 cP. A temperature of 25°C with an equilibration time of 20 s was used. The disposable folded capillary cell (DTS1070) was used for all measurements. All three parameters were measured before and after freeze-drying for nanoparticles without plasmid and after freeze-drying in particles with plasmid. Measurements were repeated in at least triplicate for each value.

Nanoparticles were also assessed visually via scanning electron microscopy (SEM). Only nanoparticles containing plasmid were imaged in the present study. Prior to SEM, samples were prepared on stands using double-sided carbon adhesive. Samples were then coated in a nanoscale layer of platinum to allow for visualisation. After coating, samples were imaged via the Tescan SEM (Tescan, Czechia). Micrographs were acquired at 2 keV, 100-pA beam current, and 10-mm working distance.

Formulation	Surfactant/Solubilizing method	Bile Acid
1	0	0
2	1% T-80	0
3	1% T-80	UDCA
4	5% T-80	UDCA
5	10% T-80	UDCA
6	5% PEG 600	UDCA
7	5% Etoh	UDCA
8	5% Etoh + 1% T-80	UDCA
9	5% Etoh + 5% PEG 600	UDCA

Fig. 1 Nanoparticle formulation preparations. Left: solubilising agents used in each formulation. F1 and F2 represent control formulations. The remaining formulations contained bile acid ursodeoxycholic acid (UDCA) with various solubilising agents. F3A–5A and 8A contain Tween-80 (T-80). F7A–9A contain ethanol (Etoh). F6A and F9A contain polyethylene gly-



col (PEG) 600 diacid. All formulations contained sodium alginate, CaCl_2 , and poly-L-lysine. Formulations were prepared in at least triplicate ($n=3$) on different occasions to confirm the consistency of the method. Right: likely method for formation of nanoparticles in solution

Toxicity studies

Toxicity was assessed through the WST-1 assay in HEI-OC1 cells (Donated by Dr Young Joon Seo). WST-1 assay was performed as per the kit insert with minor modifications. HEI-OC1 cells were cultured in Nunc EasYFlask 75-cm² flasks (Thermo Fisher, USA) at 33 °C in 10% CO₂ in Dulbecco's Modified Eagle Medium (DMEM) (Thermo Fisher, USA) supplemented with 10% Foetal Bovine Serum (FBS) (Thermo Fisher, USA). Prior to treatment, cells were passaged before being plated on a Nunc™ MicroWell™ 96-Well, Nunclon Delta-Treated, Flat-Bottom Microplate (Thermo Fisher, USA) at a concentration of 10⁵ cells/well. Cells were then allowed to establish over 24 h. Media was then removed, and the wells were washed with Phosphate Buffered Saline (PBS). Nanoparticles were serially diluted from 1 to 0.125 mg/ml in DMEM only. A total of 100 µl of these diluted formulations were then applied to wells in triplicate for each permeation of each formulation. Control wells with media only and media + cells were also prepared at this time. The 96-well plate was then incubated in the permissive conditions previously discussed. After 48 h, the plates were removed. Each well was again washed with PBS to remove residual nanoparticles. WST-1 reagent diluted 1:10 was then added to each well. The plates were then incubated for a further 4 h at 33 °C. After 4 h, the plates were removed and wrapped in foil to minimise light exposure. The plates were briefly homogenised with a plate rocker before the absorbance was read at 440 nm using the Infinite M Nano+ (Tecan, Switzerland) plate reader. The results were normalised to give a relative percentage of survival. Zero percent survival was considered to be the absorbance of the plate with media only, whilst 100% survival was the untreated plate with cells and media.

eGFP nanoparticles, transfection, and plasmid release

GFP transfection was performed using methods similar to those previously reported in the literature [39–41]. pEGFP-N1 (V012021) was purchased from NovoPro Bioscientific Inc, Shanghai, China. The vector was prepared as per manufacturer instructions and stored at –20 °C when not in use. Nanoparticles were prepared as previously discussed. However, PLL

was prepared with plasmid diluted to 20 µg/ml. The plasmid was gently brought up to room temperature before use. PLL/plasmid complex was then added to the formulation and was mixed at 1000 RPM over 60 min. Formulations were filtered, frozen, and freeze dried.

For transfection assays, HEI-OC1 cells were cultured as per previously discussed toxicity assays in 75-cm² flasks. Once cells reached 70–80% confluence they were trypsinised and diluted in DMEM supplemented with FBS to 10⁴ cells/ml. One millilitre of the diluted cells were then applied to each well of a 24-well Nunc™ Cell-Culture Treated Multidish (Thermo Fisher, USA). Cells were incubated for 24 h to allow them to establish. After 24 h, plasmid-containing formulations (F1-9) were filtered and applied to the cells at a concentration of 0.5 mg/ml. Nanoparticles were diluted in DMEM only and 1 ml was applied to each well. The plates were mixed briefly before being placed back in the incubator. After 24 h of co-incubation of plasmid nanoparticles with cells, the media was removed, and the plate was washed with PBS. DMEM supplemented with FBS was then applied. Cells were then placed back in the incubator. Transfection was then observed visually at 24, 48, and 72 h after media change using an Olympus IX-51 inverted microscope with a FITC filter.

Plasmid release studies were performed with the Quant-iT™ dsDNA Assay Kit, broad range (Thermo Fisher, USA) as per the manufacturer's instructions. Nanoparticles were prepared with plasmid as discussed previously. Particles were re-suspended at 1 mg/ml in PBS (pH = 7.2). A 10-µl aliquot was then removed and added to the quantification reagent alongside a standard e curve. Fluorescence was measured at excitation/emission of 510/527 nm using the Infinite M Nano+ plate reader. The fluorescence was compared to the standards provided in the kit to report a concentration of nucleic acid. This process was repeated at +2-, 4-, and 6-h incubation at 37 °C to demonstrate release properties over time.

Cellular metabolism and bioenergetics

Cell metabolism analysis was performed via the Seahorse XF 96 assay (Agilent, USA), using the manufacturer's methods as previously described by the laboratory [42–44]. Briefly, HEI-OC1 cells were prepared as per the previously described cellular assays.

Ninety-six hours before analysis, cells were plated at 10^5 cells/ml in 180 μ l of DMEM. The following day (48 h before analysis), nanoparticles were applied at concentrations of 0.5 and 0.25 mg/ml aseptically. Twenty-four hours prior to analysis, a sensor cartridge was hydrated and left overnight in a 37 °C incubator in the absence of CO₂. On the day of the assay, a supplemented DMEM (phenol-free) was prepared by the addition of pyruvate, glutamine, and glucose according to the manufacturer's instructions. This supplemented media was then used to carefully wash the cells, prior to degassing in a CO₂-free incubator. The supplemented DMEM was then used to resuspend lyophilised reagents supplied in the kit (oligomycin, FCCP, and rotenone and antimycin A). Whilst the cells were degassing, each reagent was then aliquoted into the appropriate well. The calibrator was run to ensure assay validity. The assay was then run as per standard operating procedures.

Statistical analysis

Experiments in this study were repeated in at least triplicate, and generally on at least two separate occasions with nanoparticles produced on different days to control for inconsistency between production. Statistical analysis was performed with the latest available version of GraphPad Prism for Windows, GraphPad Software, San Diego, California USA, www.graphpad.com. Statistical significance was calculated with a one-way ANOVA unless otherwise indicated. For line graphs, an area under the curve (AUC) analysis was performed, and statistical significance was then calculated by comparing the generated values for each formulation: * $p < 0.05$, ** $p < 0.005$, *** $p < 0.0005$, **** $p < 0.0001$.

Results

Formulation optimisation

Particle formulation involved significant optimisation. Optimisation of the method to solubilise UDCA, whilst maintaining consistent, small, and non-toxic nanoparticles presented the most significant challenge. Several solubilising agents were used in an attempt to incorporate UDCA into the nanoparticles.

Structural studies

The results of nanoparticle Zetasizer analysis are indicated in Fig. 2A–C. Figure 2A indicates particle size, Fig. 2B shows nanoparticle PDI, and Fig. 2C indicates particle charge. Control nanoparticles showed a pre-freeze-dried size of ~80 nm. After freeze-drying, this increased to 105 nm. Interestingly, this goes against the trend of the other formulations. On average, formulations shrunk by 16% after freeze-drying. The only other formulation, besides F1A to increase in size was F5A. The remaining formulations decreased in size from 5 to 57%. The control formulation however also showed a decrease in PDI after freeze-drying by 32%. Alternatively, the T-80 control F2A showed a modest increase in PDI by 36%. The remaining formulations showed more subtle variations in PDI from a 27% increase to a 20% decrease. Finally, the charge also showed significant variation after freeze-drying. Although on average there was only a modest 1% increase in charge after freeze drying, most formulations individually showed significant change.

SEM imaging of nanoparticles, as shown on the right side of Fig. 2, indicated conflicting results. Although some formulations did show nanoscale particles, there was significant amounts of “stringy” matrix. Although some formulations did show indications of nanoparticles (F1, F5, F7, F8, F9), even these showed very few particles. These images appeared to more closely resemble structures associated with hydrogels rather than nanoparticles [45].

Cytotoxicity, plasmid release, bioenergetics, and transfection

Cell cytotoxicity, as measured using the WST-1 assay, is demonstrated in Fig. 3A. Several of the formulations developed showed significant cytotoxicity towards HEI-OC1 cells. Notably, formulations containing Tween-80 to attempt to solubilise UDCA demonstrated significant toxicity at all concentrations. Given the association of increased T-80 and increased cytotoxicity, it is more likely that the increased cytotoxicity is because of T-80 rather than UDCA. Interestingly, ethanol both alone and with T-80 resulted in no significant decrease in cell survival, compared to

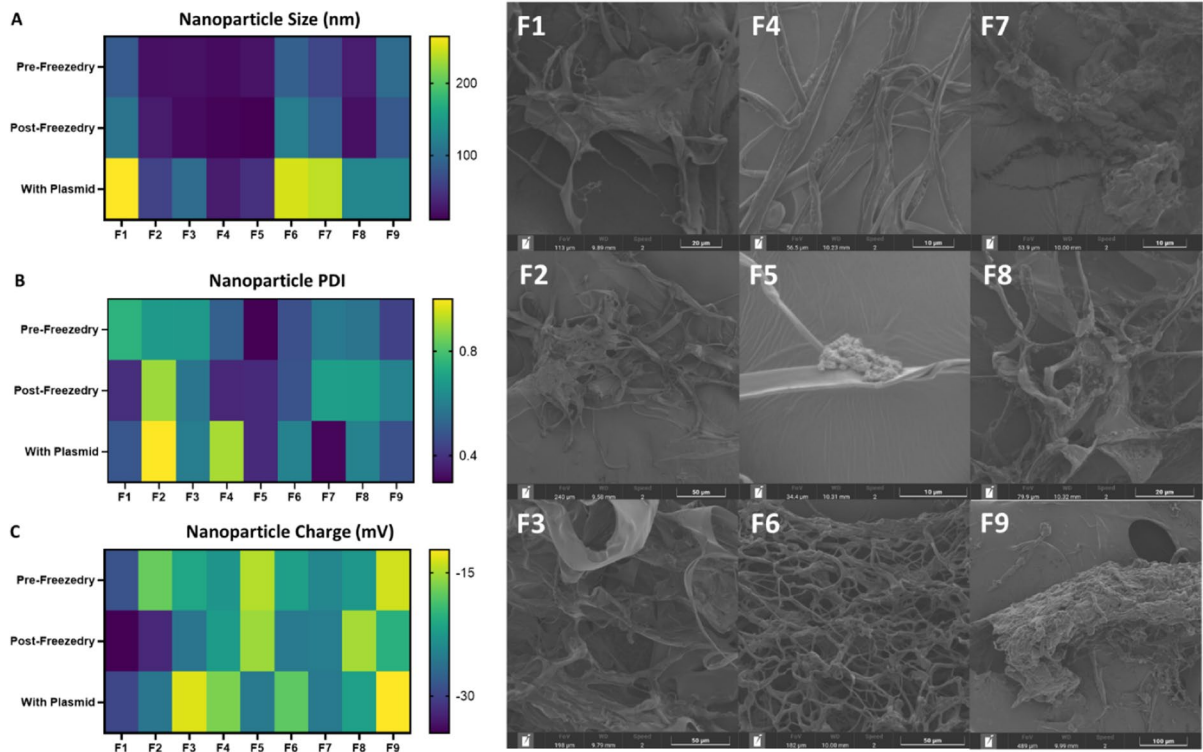


Fig. 2 Formulation physical properties. **A** Particle size (nm) pre- and post-freeze-drying process of formulations prepared in this study and post-freeze drying with plasmid. **B** Nanoparticle polydispersity index (PDI) pre- and post-freeze dry and post-freeze dry with plasmid. **C** Nanoparticle charge (mV)

pre- and post-freeze dry and post-freeze dry with plasmid. All results are reported as averages of experiments completed in at least triplicate ($n=3$). $*p<0.05$, $**p<0.005$, $***p<0.0005$, $****p<0.0001$. The right side of the figure shows scanning electron microscopy images with scale

both untreated and control formulations. Control formulation F1A also did not show significant cell death at low concentrations. Finally, ethanol with PEG 600 diacid resulted in an increase in cell survival at low concentrations compared to controls.

Plasmid-containing nanoparticles were freeze dried for 48 and 96 h to review the effects of freeze-drying on plasmid. Gene expression studies were carried out at both time points. At 96 h, there was no eGFP expression in the cells despite positive expression in the controls after freeze drying for 96 h (data not shown). Although studies do indicate that freeze drying does prolong plasmid stability [46, 47]. Previous studies have indicated that freeze drying, especially for prolonged periods with poor cryoprotection may result in plasmid degradation and reduced activity which is similar to what was seen here [48].

After freeze drying for only 48 h however, we did find limited transfection in this study as seen in

Fig. 3B. Fluorescence was only observed visually in the present study. Confirmatory methods, such as flow cytometry, were not performed as transfection was very low overall, although was greater than the use of naked plasmid (where no fluorescence was seen). Only F1, 4, 5, and 9 showed eGFP expression between 48 and 72 h after treatment. Interestingly, this corresponds to the control formulation (F1), the two formulations with the highest concentration of T-80 (F4 and F5), and the PEG+ Etoh-containing formulation (F9). This suggests that despite the high cytotoxicity of T-80 containing formulations, they still show promising transfection results. It is estimated that this transfection would be very low, likely at $<0.1\%$. Significant optimization of the nanoparticles generated in this study would be required for future use. Several approaches have previously been used to increase transfection of polymer nanoparticles. The remaining formulations did not show any GFP expression.

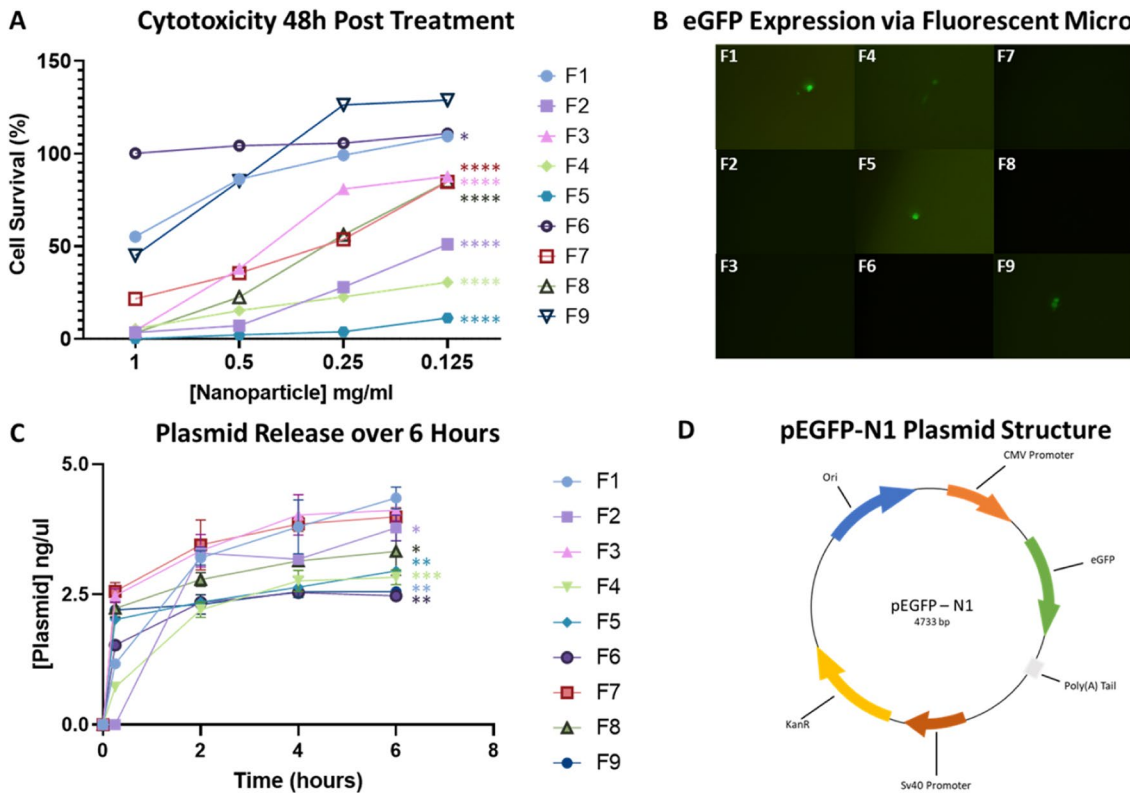


Fig. 3 WST-1 assay and plasmid release. **A** Normalised cell survival based on untreated and blank wells as reported from the WST-1 assay. Nanoparticles prepared in serial dilutions based on the mass of nanoparticles prepared in DMEM. **B** Gene expression analysis performs via visualisation of GFP

protein under fluorescent microscopy. **C** Plasmid release over 6 h in PBS (pH=7.2). **D** Structure of the plasmid used in this study. Significance comparing area under curve analysis * $p < 0.05$, ** $p < 0.005$, *** $p < 0.0005$, **** $p < 0.0001$

This low transfection is despite promising results in the plasmid release studies seen in Fig. 3C. All nanoparticle formulations showed increased plasmid release over time in PBS, with almost all formulations showing at least 2-ng/ul plasmid after 6-h incubation. The increased concentration over time suggests that plasmid was encapsulated in the nanoparticles generated in this study, if this were not the case, it would be more probable to see little to no increase in plasmid concentration over time. The structure of the pEGFP-N1 plasmid used in this study is shown in Fig. 3D.

The bioenergetic profiles generated from the Seahorse XF analyser for each formulation are displayed in Fig. 4.

The data generated via the Seahorse assay generally agrees with the WST cytotoxicity data presented in Fig. 3A. The basal respiration of formulations was

generally consistent with untreated cells, apart from F4 and F5 at 0.5 mg/ml, which showed a statistically significant ($p < 0.05$) decrease in oxygen consumption rate (OCR) as basal respiration (Fig. 4A). This reduced respiration was also demonstrated in maximal and non-mitochondrial OCR (Fig. 4B, D). These formulations also showed poor viability. Proton leak was also significantly ($p < 0.0001$) decreased in F5 at 0.5 mg/ml. Interestingly, there were significant increases in proton leak in F3, and F6 at 0.5 mg/ml and F4 at 0.25 mg/ml (Fig. 4C). There was significant variation in ATP production amongst treatment groups, with several formulations showing variation compared to the control (Fig. 4G). Glycolysis and basal proton efflux remained consistent between treatment and control groups, except for F4 and F5 (Fig. 4E–F).

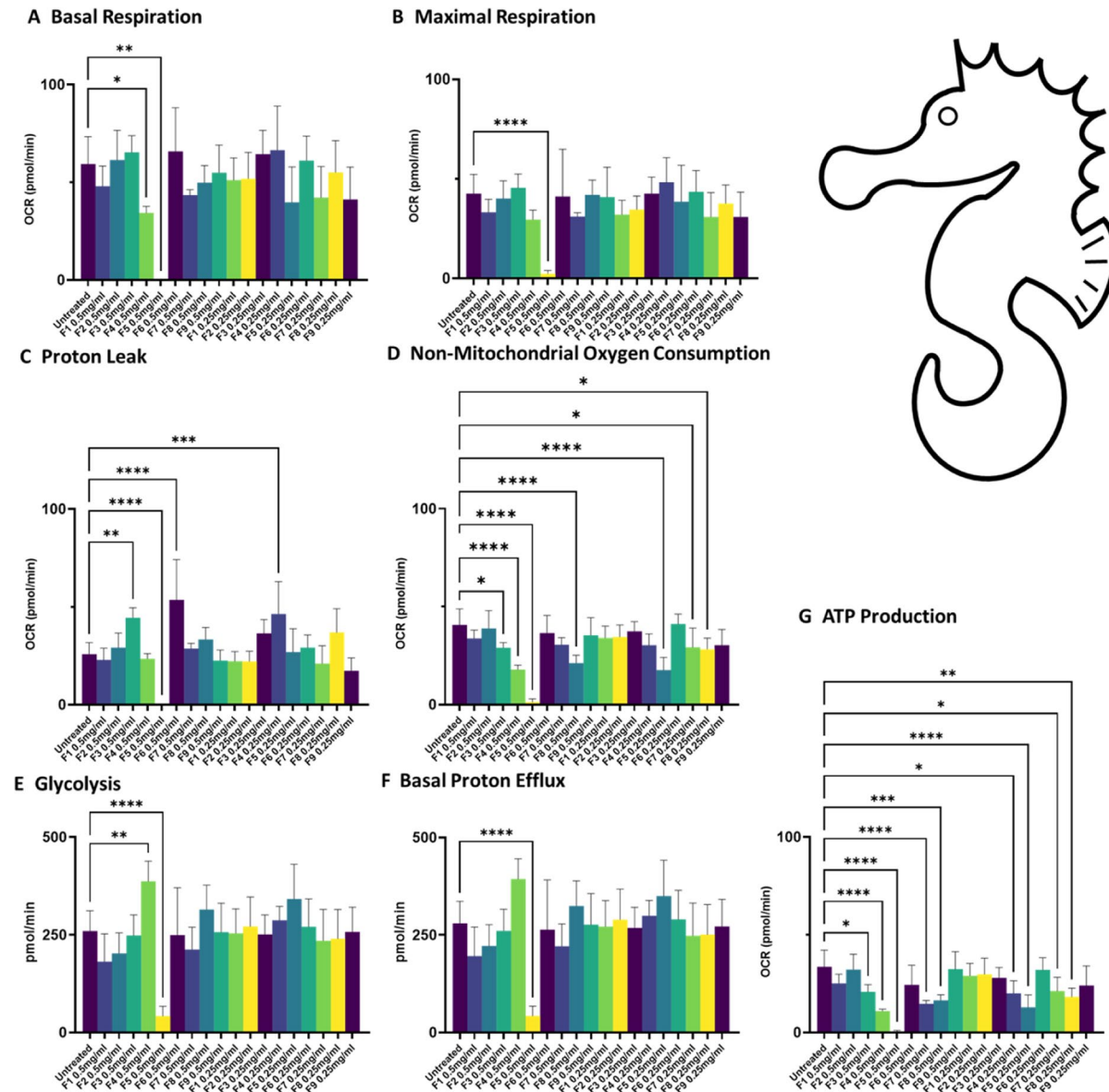


Fig. 4 Bioenergetics profiles. Bioenergetics profiles for nanoparticle formulations F1-9 in HEI-OC1 cell line without plasmid as measured by Seahorse XF analyser. Samples were analysed at both 0.5 and 0.25 mg/ml. Basal respiration, maximal

respiration, proton leak, non-mitochondrial oxygen consumption, glycolysis, basal proton efflux, and ATP production (A–G). * $p < 0.05$, ** $p < 0.005$, *** $p < 0.0005$, **** $p < 0.0001$

Discussion

Nanoparticle formulation properties initially appeared promising with small particle size, acceptable PDI, and workable charge. The nanoparticles produced in the present study represent early examples of a gene delivery system to inner ear cells. The primary goal

of this work is to develop nanoparticles suitable for direct delivery to patients. Although there are several methods for gene delivery to the cells of the inner ear, intra-tympanic injection is a commonly used technique [49]. This technique however requires nanoparticles to traverse the round window membrane (RWM) [50]. There is significant variation, based on

particle formulation, for appropriate size and charge for RWM permeation [51–53]. It has been reported that positively charged nanoparticles are more capable of permeating the RWM; however, they are also associated with more cytotoxicity compared with negatively charged nanoparticles [51]. Further studies in artificial RWM [54], ex vivo, or in vivo models would be required to understand how capable the particles produced in this study are at entering the complex inner ear.

Control nanoparticle formulation F1A showed acceptable particle size, with poor PDI. It has previously been reported that polymer particles of between 150 and 300 nm show desirable permeation across the RWM [55]. PDI is a measurement of dispersity, it has been reported that solutions with a $PDI > 0.3$ are to be considered polydisperse [56]. Maintaining mono dispersity is critical for consistency between results and for the development of a commercially viable product. The addition of T-80 reduced particle size (F1 vs F2). This reduction was not statistically significant in the pre freeze dried measurement, but it was significant ($p < 0.0001$) in the post-freeze-dried samples. The addition of UDCA resulted in a further decrease in particle size compared to the control formulation F1 and the formulation with only T-80, F2. Further, there was a statistically significant particle size decrease in all formulations compared to the control F1A except for F5A which contained only ethanol. It is well known that surfactants, such as T-80, result in a reduction of particle size for the nanoparticles [57]. The surfactant is likely lowering the surface tension of the polymer nanoparticle structure. This allows for an increase in the particle dispersion resulting in more nanoparticles of smaller size [58]. The UDCA may be acting through similar mechanisms to reduce particle size. Previous studies have demonstrated various effects of UDCA on polymer nanoparticle size [59].

The results from the SEM conflict somewhat with the data interpreted from the physical analysis. Although imaging is not an exhaustive method for confirming nano structures, few nanoparticles were identified in each formulation. Given that formulations were filtered prior to administration, it is plausible that this matrix never directly interacted with the cells. However, this may also mean that a lower amount of plasmid reached the cells and could provide some explanation for the low transfection

efficiency noted in this study. We suggest that future studies explore different ratios of SA:PLL:CaCl₂ to evaluate what effect, if any, this has on the ratio of nanoparticle to matrix.

Control formulation, F1, followed a dose-dependent cytotoxicity, with increasing concentration of nanoparticles being associated with increased toxicity. Given that F1 only contained SA, PLL, and CaCl₂, it follows that at least one of these reagents is at least somewhat toxic to the HEI-OC1 cells used. Of these, PLL has previously been shown to be cytotoxic and is thus likely the culprit [60]. It has been reported that PLL acts through intrinsic and extrinsic pathways to initiate cellular apoptosis [61]. Most other formulations showed higher cytotoxicity at all dilutions, with increasing T-80 concentration being correlated with increased toxicity, i.e. F3, F4, and F5. The addition of UDCA did somewhat mitigate this toxicity as seen when comparing F2 and F3. UDCA has known anti-apoptotic properties that may be contributing to reduced cellular death [22]. PEG-containing formulations F6A and F9 were the only nanoparticles to show improved cellular health compared to control formulation F1 via WST-1 assay. F6 showed a statistically significant improvement in cellular survival based on AUC analysis ($p < 0.05$). PEG is well known to reduce the toxicity of drugs and nanoparticles [62]. Interestingly, PEGylated nanoparticles have previously been reported to stimulate the immune system [63]. Data generated through the Seahorse assay was concordant with the WST-1 cytotoxicity assay. F5 and F4 showed particularly poor respiration, both mitochondrial and basal. This suggests mitochondrial dysfunction may be a causal or consequential mechanism of cell death within these cells after treatment.

Although the present study was performed in vitro, there are several aspects regarding potential in vivo delivery that should be considered concurrently. Degradation of nanoparticles is a key consideration within the sensitive inner ear. Alginate nanoparticles formed via ionotropic gelation are known to degenerate in a pH dependent, but predictable, manner [64]. Although mammals lack the required enzyme to degrade alginate to its monomers, it is generally thought, that over time, alginate will progressively lose its cation (in this case sodium), which will result in the alginate dissolving [65]. Alginate's properties can be tuned to modify the time it takes for degradation to occur [66]. The soluble alginate can then be

removed from the ear through normal cellular processes and excreted. PLL, the other polymer used in this study, can be degraded enzymatically before being exported out of the ear and excreted [67]. Further studies *in vivo*, within the inner ear specifically are required to understand with more certainty how these processes occur. Additionally, although toxicity studies were extensively explored in this study, interactions with organelles, such as the stapes, are important to consider as the inner ear cells used in this study may not be representative of all cell types. Although no studies have evaluated the toxicity of the nanoparticles developed in this study *in vivo*, the individual components have been evaluated. For example, alginate has been shown to be non-toxic within the inner ear of mouse models [68]. There are concerns about toxicity associated with PLL [69]; however, further studies are needed to evaluate if there exists a safe *in vivo* concentration for inner ear delivery. Further, how nanoparticles may affect sound transmission through the bony and membranous labyrinth should also be considered. Although some studies have demonstrated that nanoparticles do modify sound transmission through aqueous phases [70], the significance of this *in vivo* remains uncertain. Finally, non-invasive quantification of hearing modification would also be critical in any potential future *in vivo* experiments. Behavioural studies for example are one common method of evaluating the degree of hearing loss in mouse models [71].

Plasmid release showed strong agreement between formulations with a steady but noticeable increase in plasmid concentration over the course of 6 h. No significant change in concentration was noted after this point so no further data was collected. As per Fig. 3B, there was no significant increase in plasmid release compared with control formulation F1. All formulations rather showed a statistically significant decrease in release over time except F3 and F7. The slightly delayed release of plasmid demonstrated by these nanoparticles would be useful for the delivery of plasmid to the inner ear. The slight delay would allow for the nanoparticles to permeate into the inner ear prior to the release of the plasmid, protecting it from degradation. Previous studies have indicated pH dependent release from similarly formulated nanoparticles. For example, PLL nanoparticles have previously been shown to have pH mediated drug release, with increased release at lower pH [72].

Unfortunately, transfection in HEI-OC1 cells was very poor, with only four formulations showing any transfection despite positive controls producing results. We would estimate transfection efficiency to be <1% in the present study. Only F1, 4, 5, and 9 demonstrated successful transfection of HEI-OC1 cells as confirmed qualitatively by fluorescent microscopy. Control formulation F1 is similar to other formulations that have previously been shown to successfully deliver nucleic acid *in vivo* [11]. However, very few studies available in the literature report the delivery of plasmids with alginate/PLL nanoparticles, particularly to inner ear cells. Interestingly, F4 and 5 correspond with increasing T-80 concentration and increased cytotoxicity. Suggesting that despite higher toxicity, these formulations were capable of improved transfection. It is hypothesised that T-80 may be improving gene delivery via one of two methods. One, the T-80 may be spontaneously forming liposomes or lipid nanoparticle-like structures independent of the polymers, in conjunction with UDCA to deliver plasmid [73]. Alternatively, previous studies have shown that T-80 improves cellular uptake of nanoparticles and thus may have contributed to the increased plasmid expression seen [74]. The addition of UDCA alone to nanoparticles however did not appear to have any significant effect on transfection (F2 vs F3).

Given the poor transfection efficiency of the nanoparticles presented in this study, it may be prudent to explore the transfection efficiency in a range of different cell lines in future studies. It is common for nanoparticles to show different levels of transfection efficiency in different cell lines [75]. Alternatively, modification of the nanoparticles to improve delivery may increase eGFP expression in the HEI-OC1 cells. For example, studies have shown that strategies including modulating polymer properties, stability modifications, buffering modifications, and the use of cell-penetrating peptides have all been shown to improve transfection efficiency [76–78]. Further, to improve cell targeted specific release, various methods, including the conjugation of antibodies may be employed [79]. Given the preliminary nature of this study, such methods were not employed here; however, they could be applied to the nanoparticles prepared in this study.

To place this research into some context, we have briefly evaluated some other methods for nanocapsulation of plasmid for auditory delivery. A summary of this data is provided in Table 1. Given the

Table 1 Comparison of nanotechnology based gene delivery for the inner ear. A summary of some of the delivery methods reported in the literature for gene therapy within the inner ear

Components	Synthesis method	Size (nm)	Charge (mV)	Toxicity	Transfection efficiency	Citation
Cell penetrating peptides \pm dexamethasone	Self-assembly	90	-	Toxicity at 0.05–0.1 mg/ml	Greater transfection efficiency than lipofectamine control	[80]
Polyethyleneimine-polyethylene glycol	Aggregation	-	-	Lower toxicity than control	Increased gene expression in vitro and in vivo	[81, 82]
Poly D,L-lactic-co-glycolic acid	Emulsion	184	-27	No toxicity noted at <800 μ g/ml	Comparable to control in HEI-OC1 cells	[83]
Poly-L-lysine/alginate \pm taurocholic acid	Ionic gelation	100–250	-20–40	Increased toxicity at 1 mg/ml	Poor transfection efficiency	[21]
Polyamidoamine dendrimer	-	132	31	-	Selective transfection of auditory hair cells	[84]

emerging nature of gene therapy, there were few comparable studies available in the literature.

Conclusion

To conclude, this study developed and characterised various nanoparticle formulations for potential gene delivery in inner ear cell lines. Formulations were evaluated for their properties, including charge, size, polydispersity, cytotoxicity, plasmid release, and transfection capability. The results suggest that nanoparticle formulations containing surfactants, such as T-80 and the bile acid, UDCA was able to potentially reduce particle size and modify plasmid release and transfection. Further, PEG-containing nanoparticles showed potential improvement in cellular health compared to the other formulations. Transfection efficiency in the HEI-OC1 cell line was, however, low. Low transfection is a common issue associated with polymer nanoparticles. Thus, further optimisation of these nanoparticles is required for efficient gene delivery within the inner ear. Despite this, the authors believe that polymer nanotechnology still represents a novel and potentially viable method for the efficient delivery of gene therapy products to the inner ear, primarily due to their well-studied safety profiles and customisability. Further studies could investigate these, or similar polymer nanoparticles for in vivo or ex vivo delivery in combination with modified polymers or additional excipients to better understand their release properties.

Acknowledgements The authors would like to acknowledge the Australian Research Training Program Scholarship for their support, in addition to the Australian Postgraduate Award and Curtin Research Scholarship. The authors also acknowledged the use of laboratory equipment and the scientific and technical assistance of the Curtin University Electron Microscope Facility, which has been partially funded by the University, State, and Commonwealth Governments. The authors also acknowledge the use of equipment and the technical staff from the Curtin Health Innovation Research Institute (CHIRI) without which this work would not be possible. The authors are also very grateful to Dr Young Joon Seo (Yonsei University Wonju College of Medicine) and Prof Federico Kalinec (UCLA) for the auditory cell line used in this study.

Funding Open Access funding enabled and organized by CAUL and its Member Institutions. This work is partially supported by the European Union Horizon 2020 research project and innovation program under the Marie Skłodowska-Curie Grant Agreement No 872370. This work is also supported partially by Curtin Faculty ORS-WAHAI Consortium, via the Australian National Health and Medical Research Fund (APP9000597).

Data availability The datasets generated and/or analysed during the current study are not publicly available but are available from the corresponding author on reasonable request due to pending commercialization limitations.

Declarations

Conflict of interest The authors declare no competing interests.

Open Access This article is licensed under a Creative Commons Attribution 4.0 International License, which permits use, sharing, adaptation, distribution and reproduction in any medium or format, as long as you give appropriate credit to the original author(s) and the source, provide a link to the Creative Commons licence, and indicate if changes were made. The

images or other third party material in this article are included in the article's Creative Commons licence, unless indicated otherwise in a credit line to the material. If material is not included in the article's Creative Commons licence and your intended use is not permitted by statutory regulation or exceeds the permitted use, you will need to obtain permission directly from the copyright holder. To view a copy of this licence, visit <http://creativecommons.org/licenses/by/4.0/>.

References

- Haile LM, Kamenov K, Briant PS, Orji AU, Steinmetz JD, Abdoli A et al (2021) Hearing loss prevalence and years lived with disability, 1990–2019: findings from the Global Burden of Disease Study 2019. *Lancet* 397(10278):996–1009
- Li W, Zhao Z, Lu Z, Ruan W, Yang M, Wang D (2022) The prevalence and global burden of hearing loss in 204 countries and territories, 1990–2019. *Environ Sci Pollut Res Int* 29(8):12009–12016
- Foster T, Lewkowicz M, Quintas C, Ionescu CM, Jones M, Wagle SR, ... Al-Salami H (2023) Novel nanoencapsulation technology and its potential role in bile acid-based targeted gene delivery to the inner ear. *Small* 19(8):2204986
- Omichi R, Shibata SB, Morton CC, Smith RJ (2019) Gene therapy for hearing loss. *Hum Mol Genet* 28(R1):R65–R79
- Chien WW, Monzack EL, McDougald DS, Cunningham LL (2015) Gene therapy for sensorineural hearing loss. *Ear Hear* 36(1):1–7
- White PM, Doetzlhofer A, Lee YS, Groves AK, Segil N (2006) Mammalian cochlear supporting cells can divide and trans-differentiate into hair cells. *Nature* 441(7096):984–987
- Hao J, Li SK (2019) Inner ear drug delivery: recent advances, challenges, and perspective. *Eur J Pharm Sci* 126:82–92
- Valentini C, Szeto B, Kysar JW, Lalwani AK (2020) Inner ear gene delivery: vectors and routes. *Hear Balance Commun* 18(4):278–285
- Sacheli R, Delacroix L, Vandenaekerveken P, Nguyen L, Malgrange B (2013) Gene transfer in inner ear cells: a challenging race. *Gene Ther* 20(3):237–247
- Maguire CA, Corey DP (2020) Viral vectors for gene delivery to the inner ear. *Hear Res* 394:107927
- Ferreiro MG, Tillman LG, Hardee G, Bodmeier R (2002) Alginate/poly-L-lysine microparticles for the intestinal delivery of antisense oligonucleotides. *Pharm Res* 19:755–764
- Ferreiro MG, Tillman L, Hardee G, Bodmeier R (2002) Characterization of alginate/poly-L-lysine particles as antisense oligonucleotide carriers. *Int J Pharm* 239(1–2):47–59
- Atkinson PJ, Wise AK, Flynn BO, Nayagam BA, Richardson RT (2014) Hair cell regeneration after ATOH1 gene therapy in the cochlea of profoundly deaf adult guinea pigs. *PLoS ONE* 9(7):e102077
- Dabdoub A, Puligilla C, Jones JM, Fritzsich B, Cheah KS, Pevny LH et al (2008) Sox2 signaling in prosensory domain specification and subsequent hair cell differentiation in the developing cochlea. *Proc Natl Acad Sci* 105(47):18396–18401
- Ahmed M, Wong EY, Sun J, Xu J, Wang F, Xu P-X (2012) Eya1-Six1 interaction is sufficient to induce hair cell fate in the cochlea by activating Atoh1 expression in cooperation with Sox2. *Dev Cell* 22(2):377–390
- Atkinson PJ, Huarcaya Najarro E, Sayyid ZN, Cheng AG (2015) Sensory hair cell development and regeneration: similarities and differences. *Development* 142(9):1561–1571
- Mooranian A, Foster T, Ionescu CM, Carey L, Walker D, Jones M et al (2021) The effects of primary unconjugated bile acids on nanoencapsulated pharmaceutical formulation of hydrophilic drugs: pharmacological implications. *Drug Des Devel Ther* 15:4423
- Mooranian A, Foster T, Ionescu CM, Walker D, Jones M, Wagle SR et al (2021) Enhanced bilosomal properties resulted in optimum pharmacological effects by increased acidification pathways. *Pharmaceutics* 13(8):1184
- Mooranian A, Ionescu CM, Wagle SR, Kovacevic B, Walker D, Jones M et al (2021) Probuocol pharmacological and bio-nanotechnological effects on surgically transplanted graft due to powerful anti-inflammatory, anti-fibrotic and potential bile acid modulatory actions. *Pharmaceutics* 13(8):1304
- Foster T, Ionescu C, Walker D, Jones M, Wagle S, Kovacevic B et al (2021) Chemotherapy-induced hearing loss: the applications of bio-nanotechnologies and bile acid-based delivery matrices. *Ther Deliv* 12(10):723–737
- Foster T, Ionescu CM, Jones M, Wagle SR, Kovacevic B, Lim P, ... Al-Salami H (2023) Poly-L-lysine as a crosslinker in bile acid and alginate nanoaggregates for gene delivery in auditory cells. *Nanomedicine* 18(19):1247–1260
- Rodrigues CM, Steer CJ (2001) The therapeutic effects of ursodeoxycholic acid as an anti-apoptotic agent. *Expert Opin Investig Drugs* 10(7):1243–1253
- Abdulrab S, Al-Maweri S, Halboub E (2020) Ursodeoxycholic acid as a candidate therapeutic to alleviate and/or prevent COVID-19-associated cytokine storm. *Med Hypotheses* 143:109897
- Ward JB, Lajczak NK, Kelly OB, O'Dwyer AM, Giddam AK, Ní Gabhann J et al (2017) Ursodeoxycholic acid and lithocholic acid exert anti-inflammatory actions in the colon. *Am J Physiol Gastrointest Liver Physiol* 312(6):G550–G8
- Al-Salami H, Mamo J, Mooranian A, Negrulj R, Lam V, Elahy M et al (2017) Long-term supplementation of microencapsulated ursodeoxycholic acid prevents hypertension in a mouse model of insulin resistance. *Exp Clin Endocrinol Diabetes* 125(01):28–32
- Mooranian A, Negrulj R, Arfuso F, Al-Salami H (2016) Characterization of a novel bile acid-based delivery platform for microencapsulated pancreatic β -cells. *Artif Cells Nanomed Biotechnol* 44(1):194–200
- Hofmann A (1994) Pharmacology of ursodeoxycholic acid, an enterohepatic drug. *Scand J Gastroenterol* 29(sup204):1–15

28. Ventura C, Tirendi S, Puglisi G, Bousquet E, Panza L (1997) Improvement of water solubility and dissolution rate of ursodeoxycholic acid and chenodeoxycholic acid by complexation with natural and modified β -cyclodextrins. *Int J Pharm* 149(1):1–13
29. Okonogi S, Yonemochi E, Oguchi T, Puttipipatkachorn S, Yamamoto Keiji (1997) Enhanced dissolution of ursodeoxycholic acid from the solid dispersion. *Drug Dev Ind Pharm* 23(11):1115–21
30. Xie Y, Chen Z, Su R, Li Y, Qi J, Wu W et al (2017) Preparation and optimization of amorphous ursodeoxycholic acid nano-suspensions by nanoprecipitation based on acid-base neutralization for enhanced dissolution. *Curr Drug Deliv* 14(4):483–491
31. Choukaife H, Doolaanea AA, Alfatama M (2020) Alginate nanoformulation: influence of process and selected variables. *Pharmaceuticals* 13(11):335
32. Mokhtari S, Jafari SM, Assadpour E (2017) Development of a nutraceutical nano-delivery system through emulsification/internal gelation of alginate. *Food Chem* 229:286–295
33. Majimbi M, Brook E, Galetti P, Eden E, Al-Salami H, Mooranian A et al (2021) Sodium alginate microencapsulation improves the short-term oral bioavailability of cannabidiol when administered with deoxycholic acid. *PLoS ONE* 16(6):e0243858
34. Dai Y, Zhou R, Liu L, Lu Y, Qi J, Wu W (2013) Liposomes containing bile salts as novel ocular delivery systems for tacrolimus (FK506): in vitro characterization and improved corneal permeation. *Int J Nanomedicine* 8:1921–1934
35. Bashyal S, Seo J-E, Keum T, Noh G, Choi YW, Lee S (2018) Facilitated permeation of insulin across TR146 cells by cholic acid derivatives-modified elastic bilosomes. *Int J Nanomed* 13:5173
36. Mathavan S, Chen-Tan N, Arfuso F, Al-Salami H (2016) A comprehensive study of novel microcapsules incorporating gliclazide and a permeation enhancing bile acid: hypoglycemic effect in an animal model of Type-1 diabetes. *Drug Deliv* 23(8):2869–2880
37. Carey L, Walker D, Jones M, Ionescu C, Wagle S, Kovacevic B et al (2021) Bile acid permeation enhancement for inner ear cochlear drug pharmacological uptake: bio-nanotechnologies in chemotherapy-induced hearing loss. *Ther Deliv* 12(12):807–819
38. Mooranian A, Zamani N, Mikov M, Goločorbin-Kon S, Stojanovic G, Arfuso F et al (2020) A second-generation micro/nano capsules of an endogenous primary un-metabolised bile acid, stabilized by Eudragit-alginate complex with antioxidant compounds. *Saudi Pharm J* 28(2):165–171
39. Ishii T, Okahata Y, Sato T (2001) Mechanism of cell transfection with plasmid/chitosan complexes. *Biochim Biophys Acta (BBA) Biomembr* 1514(1):51–64
40. Amin ZR, Rahimizadeh M, Eshghi H, Dehshahri A, Ramezani M (2013) The effect of cationic charge density change on transfection efficiency of poly(ethyleneimine). *Iran J Basic Med Sci* 16(2):150
41. van de Wetering P, Cherng J-Y, Talsma H, Hennink WE (1997) Relation between transfection efficiency and cytotoxicity of poly (2-(dimethylamino) ethyl methacrylate)/plasmid complexes. *J Control Release* 49(1):59–69
42. Kovacevic B, Ionescu CM, Jones M, Wagle SR, Lewkowicz M, Đanić M et al (2022) The effect of deoxycholic acid on chitosan-enabled matrices for tissue scaffolding and injectable nanogels. *Gels* 8(6):358
43. Kovacevic B, Ionescu CM, Wagle SR, Jones M, Lewkowicz M, Wong EY et al (2023) Impact of novel Teflon-DCA nanogel matrix on cellular bioactivity. *J Pharm Sci* 112(3):700–707
44. Mooranian A, Jones M, Ionescu CM, Walker D, Wagle SR, Kovacevic B et al (2021) Advancements in assessments of bio-tissue engineering and viable cell delivery matrices using bile acid-based pharmacological biotechnologies. *Nanomaterials* 11(7):1861
45. Barker K, Rastogi SK, Dominguez J, Cantu T, Brittain W, Irvin J et al (2016) Biodegradable DNA-enabled poly(ethylene glycol) hydrogels prepared by copper-free click chemistry. *J Biomater Sci Polym Ed* 27(1):22–39
46. Lee H, Jiang D, Pardridge WM (2020) Lyoprotectant optimization for the freeze-drying of receptor-targeted trojan horse liposomes for plasmid DNA delivery. *Mol Pharm* 17(6):2165–2174
47. Weißbecker C, Buscot F, Wubet T (2017) Preservation of nucleic acids by freeze-drying for next generation sequencing analyses of soil microbial communities. *J Plant Ecol* 10(1):81–90
48. Poxon SW, Hughes JA (2000) The effect of lyophilization on plasmid DNA activity. *Pharm Dev Technol* 5(1):115–122
49. Herraiz C, Aparicio JM, Plaza G (2010) Intratympanic drug delivery for the treatment of inner ear diseases. *Acta Otorrinolaringol (English Edition)* 61(3):225–232
50. Banerjee A, Parnes LS (2004) The biology of intratympanic drug administration and pharmacodynamics of round window drug absorption. *Otolaryngol Clin North Am* 37(5):1035–1051
51. Liu H, Chen S, Zhou Y, Che X, Bao Z, Li S et al (2013) The effect of surface charge of glycerol monooleate-based nanoparticles on the round window membrane permeability and cochlear distribution. *J Drug Target* 21(9):846–854
52. Lin Y-C, Shih C-P, Chen H-C, Chou Y-L, Sytwu H-K, Fang M-C et al (2021) Ultrasound microbubble-facilitated inner ear delivery of gold nanoparticles involves transient disruption of the tight junction barrier in the round window membrane. *Front Pharmacol* 12:689032
53. Buckiová D, Ranjan S, Newman TA, Johnston AH, Sood R, Kinnunen PK et al (2012) Minimally invasive drug delivery to the cochlea through application of nanoparticles to the round window membrane. *Nanomedicine* 7(9):1339–1354
54. Santimetaneedol A, Wang Z, Arteaga D, Aksit A, Prevo-teau C, Yu M et al (2019) Small molecule delivery across a perforated artificial membrane by thermoreversible hydrogel poloxamer 407. *Colloids Surf B Biointerfaces* 182:110300
55. Cai H, Liang Z, Huang W, Wen L, Chen G (2017) Engineering PLGA nano-based systems through understanding the influence of nanoparticle properties and cell-penetrating peptides for cochlear drug delivery. *Int J Pharm* 532(1):55–65

56. Danaei M, Dehghankhold M, Ataei S, Hasanzadeh Davarani F, Javanmard R, Dokhani A et al (2018) Impact of particle size and polydispersity index on the clinical applications of lipidic nanocarrier systems. *Pharmaceutics* 10(2):57
57. Nasef AM, Gardouh AR, Ghorab MM (2015) Polymeric nanoparticles: influence of polymer, surfactant and composition of manufacturing vehicle on particle size. *World J Pharm Pharm Sci* 3(12):2308–2322
58. Harikrishnan A, Dhar P, Agnihotri PK, Gedupudi S, Das SK (2017) Effects of interplay of nanoparticles, surfactants and base fluid on the surface tension of nanocolloids. *Eur Phys J E* 40:1–14
59. Dalpiaz A, Contado C, Mari L, Perrone D, Pavan B, Paganetto G et al (2014) Development and characterization of PLGA nanoparticles as delivery systems of a pro-drug of zidovudine obtained by its conjugation with ursodeoxycholic acid. *Drug Deliv* 21(3):221–232
60. Isaksson K, Åkerberg D, Posaric-Bauden M, Andersson R, Tingstedt B (2014) In vivo toxicity and biodistribution of intraperitoneal and intravenous poly-L-lysine and poly-L-lysine/poly-L-glutamate in rats. *J Mater Sci Mater Med* 25:1293–1299
61. Paul A, Eun C-J, Song JM (2014) Cytotoxicity mechanism of non-viral carriers polyethylenimine and poly-L-lysine using real time high-content cellular assay. *Polymer* 55(20):5178–5188
62. Greenwald R (2001) PEG drugs: an overview. *J Control Release* 74(1–3):159–171
63. Karabasz A, Szczepanowicz K, Cierniak A, Mezyk-Kopec R, Dyduch G, Szczech M, ... Bzowska M (2019) In vivo studies on pharmacokinetics, toxicity and immunogenicity of polyelectrolyte nanocapsules functionalized with two different polymers: poly-L-glutamic acid or PEG. *Int J Nanomedicine* 14:9587–9602
64. Bajpai S, Sharma S (2004) Investigation of swelling/degradation behaviour of alginate beads crosslinked with Ca²⁺ and Ba²⁺ ions. *React Funct Polym* 59(2):129–140
65. Augst AD, Kong HJ, Mooney DJ (2006) Alginate hydrogels as biomaterials. *Macromol Biosci* 6(8):623–633
66. Barceló X, Eichholz KF, Garcia O, Kelly DJ (2022) Tuning the degradation rate of alginate-based bioinks for bioprinting functional cartilage tissue. *Biomedicines* 10(7):1621
67. Ren K, Ji J, Shen J (2006) Construction and enzymatic degradation of multilayered poly-L-lysine/DNA films. *Biomaterials* 27(7):1152–1159
68. Alvi SA, Nelson-Brantley J, Staecker H (2018) Alginate ototoxicity in the mouse model. *Otolaryngol Head Neck Surg* 159(4):733–738
69. Zhou H, Ma X, Liu Y, Dong L, Luo Y, Zhu G et al (2015) Linear polyethylenimine-plasmid DNA nanoparticles are ototoxic to the cultured sensory epithelium of neonatal mice. *Mol Med Report* 11(6):4381–4388
70. De Francesco A, Scaccia L, Formisano F, Guarini E, Bafle U, Nykypanchuk D et al (2023) The effect of embedded nanoparticles on the phonon spectrum of ice: an inelastic X-ray scattering study. *Nanomaterials* 13(5):918
71. Longenecker RJ, Galazyuk AV (2011) Development of tinnitus in CBA/CaJ mice following sound exposure. *J Assoc Res Otolaryngol* 12(5):647–658
72. Yang DH, Kim HJ, Park K, Kim JK, Chun HJ (2018) Preparation of poly-L-lysine-based nanoparticles with pH-sensitive release of curcumin for targeted imaging and therapy of liver cancer in vitro and in vivo. *Drug Deliv* 25(1):950–960
73. Kronberg B, Dahlman A, Carlfors J, Karlsson J, Artursson P (1990) Preparation and evaluation of sterically stabilized liposomes: colloidal stability, serum stability, macrophage uptake, and toxicity. *J Pharm Sci* 79(8):667–671
74. Tahara K, Yamamoto H, Kawashima Y (2010) Cellular uptake mechanisms and intracellular distributions of polysorbate 80-modified poly (D, L-lactide-co-glycolide) nanospheres for gene delivery. *Eur J Pharm Biopharm* 75(2):218–224
75. Abdellatif AA, Tolba NS, Alsharidah M, Al Rugaie O, Bouazzaoui A, Saleem I et al (2022) PEG-4000 formed polymeric nanoparticles loaded with cetuximab down-regulate p21 & stathmin-1 gene expression in cancer cell lines. *Life Sci* 295:120403
76. Mansouri S, Lavigne P, Corsi K, Benderdour M, Beaumont E, Fernandes JC (2004) Chitosan-DNA nanoparticles as non-viral vectors in gene therapy: strategies to improve transfection efficacy. *Eur J Pharm Biopharm* 57(1):1–8
77. Urello MA, Xiang L, Colombo R, Ma A, Joseph A, Boyd J et al (2020) Metabolite-based modification of poly (L-lysine) for improved gene delivery. *Biomacromol* 21(9):3596–3607
78. Cheng CJ, Saltzman WM (2011) Enhanced siRNA delivery into cells by exploiting the synergy between targeting ligands and cell-penetrating peptides. *Biomaterials* 32(26):6194–6203
79. Juan A, Cimas FJ, Bravo I, Pandiella A, Ocaña A, Alonso-Moreno C (2020) An overview of antibody conjugated polymeric nanoparticles for breast cancer therapy. *Pharmaceutics* 12(9):802
80. Yoon JY, Yang KJ, Park SN, Kim DK, Kim JD (2016) The effect of dexamethasone/cellpenetrating peptide nanoparticles on gene delivery for inner ear therapy. *Int J Nanomedicine* 11:6123–6134
81. Chen G-G, Mao M, Qiu L-Z, Liu Q-M (2015) Gene transfection mediated by polyethyleneimine-polyethylene glycol nanocarrier prevents cisplatin-induced spiral ganglion cell damage. *Neural Regen Res* 10(3):425
82. Chen G-g, Xu Y-I (2014) Polyethylenimine-polyethylene glycol as a gene transfer vector for spiral ganglion cells in vitro. *Chinese J Tissue Eng Res* 18(21):3345
83. Youm I, West MB, Li W, Du X, Ewert DL, Kopke RD (2017) siRNA-loaded biodegradable nanocarriers for therapeutic MAPK1 silencing against cisplatin-induced ototoxicity. *Int J Pharm* 528(1–2):611–623
84. Wu N, Li M, Chen Z-T, Zhang X-B, Liu H-Z, Li Z et al (2013) In vivo delivery of Atoh1 gene to rat cochlea using a dendrimer-based nanocarrier. *J Biomed Nanotechnol* 9(10):1736–1745

Publisher's Note Springer Nature remains neutral with regard to jurisdictional claims in published maps and institutional affiliations.